HU8105501

KFKI-1981-08

J. GYULAI

RUTHERFORD BACKSCATTERING SPECTROMETRY

Hungarian Academy of Sciences

CENTRAL RESEARCH INSTITUTE FOR PHYSICS

BUDAPEST

KFKI-1981-08

RUTHERFORD BACKSCATTERING SPECTROMETRY

J. Gyulai

Central Research Institute for Physics
H-1525 Budapest 114, P.O.B. 49, Hungary

Submitted to Proceedings of Summer School on Surface Physics, Varna, 1980, Pergamon Press

HU ISSN 0368 5330
ISBN 963 371 786 X

ABSTRACT

Bases of Rutherford ion backscattering and its combination with channeling effect technique, is reviewed. This combined method is recently referred to as Backscattering Spectrometry. The paper deals with measurement of chemical composition, detection of crystal defects etc. Comparison with other surface analysis methods is also given. The review was delivered as a lecture during the "International School for Surface Physics" /Varna, Bulgaria, Sep. 18 - Oct. 20, 1980/.

АННОТАЦИЯ

Рассматривается метод резерфордовского рассеяния, скомбинированный с эффектом каналирования. Этот комбинированный метод в настоящее время известен под общим названием "Спектрометрия обратного рассеяния". Он включает в себя измерение химического состава, определение дефектов кристаллической решетки и т.д. Приводится сравнение с другими методами анализа тонких пленок. Обзор был включен в курс лекций, прочитанных в рамках "Международной школы физики поверхности" /Варна, Болгария, 18 сент. - 20 окт. 1980 г./.

KIVONAT

A Rutherford ionvisszaszórás és annak a csatornahatással kombinált változata - közös néven Backscattering Spectrometry, azaz Visszaszórásos Spektrometria - alapjait ismerteti az összefoglaló. Kitér a kémiai összetétel, rácshibák stb. mérésének problémáira. Összehasonlítja a módszert más vékonyréteg analitikai eljárásokkal. A cikk előadás formájában hangzott el a "Nemzetközi Felületfizikai Iskolán" /Várna, Bulgária, 1980, szept.18.-okt.20./.

1. INTRODUCTION

The market for quantitative analysis, both structural and chemical, is increasing. More and more sophisticated structures of semiconductors, dielectrics or metals are used in technologies, and the knowledge of vertical and horizontal structure is of utmost importance. The presence of detrimental impurities or defects should also be detected.

This need caused the boom of new types of analytical techniques. Practically, all sorts of interactions between photons, particles and the condensed matter were explored whether information could be gained from the end products on the undisturbed state. Therefore, all combinations of electron-electron, ion-electron, X-ray-electron etc., bear different names as analytical techniques and, also, additional "tricks", e.g. layer removal by sputtering are included, leading to new possibilities. Looking into papers, also into the enormous number of reviews, it is almost impossible to say, which method is more sensitive, or more widely applicable, because "sensitivity" bears a lot of ambiguity. And tough systems, or problematic analyses are seldom di..played in reviews advertising one or the other method. Every method can show a few examples, where their advantageous properties will win. Trace elements in ppb concentrations will be "determined" by SIMS (Secondary Ion Mass Spectrometry), but quantitizing the results or, at least, say safely that the surfaces, interfaces, ionization yields or selective sputtering did not cause any artefacts, is still behind the horizon.

Transmission electron microscope (TEM) can detect about a thousand atoms in a precipitate, but this doesnot involve that TEM is "sensitive". This limit is a consequence of good focussing and only moderate sensitivity (a BS with a similarly focussed ion beam would be much more sensitive).

Electron microprobes suffer from low stopping (deep penetration) and, therefore, lower sensitivities in near-surface studies compared to ion excited X-ray analysis (IEX). In this latter the small background from bremsstrahlung is one more advantage. But, as it was told, today electrons can be better focussed. If chemical bonds are quantities of interest, only few methods count.

It is easy to summarize demands for an "ideal" technique and to tell what compromise must be done (Table I).

Table I

Demand	or, at least,
selective to all elements	to important combinations
sensitive down to, say, 10^7 total # of atoms/cm^2	no matrix effect
sensitive to local potential	to some chemistry
structural imaging possible	be structure sensitive
resolution in three dimension (imaging)	or two, or one dimensional profiling
absolute scales	easy calibration
in situ and dynamic measurement	fast, automated
weak disturbance in target (non-destructive)	reproducible layer removal
easy to interpret	reasonably simple model
no artefacts	easy to screen out using complementary techniques
same equipment for different techniques	easy to combine
inexpensive	less than $300 k

It is the Rutherford backscattering spectrometry (BS), which in one matches mostly the requirements, though generally not with a high excellency. It gives a fast, non-destructive analysis on structure and absolute elemental composition as function of depth. Systems with nearly equal atomic masses are, however, inaccessible to BS. But, as it needs the same equipment (apart from detectors) as IEX and the so-called ion-induced nuclear reaction (IINR) analysis, most structures can be analyzed by "nuclear techniques".

As it will be shown, the directness and the diversity of the information that makes BS so unique.

Fig. 1 displays the different uses of ions of broad energy and dose range. We classify these uses as "machining" (-▸-▸-▸-), intentional change of proporties(●—●—●) and analysis (—·—·—).
Let's focus on analysis.

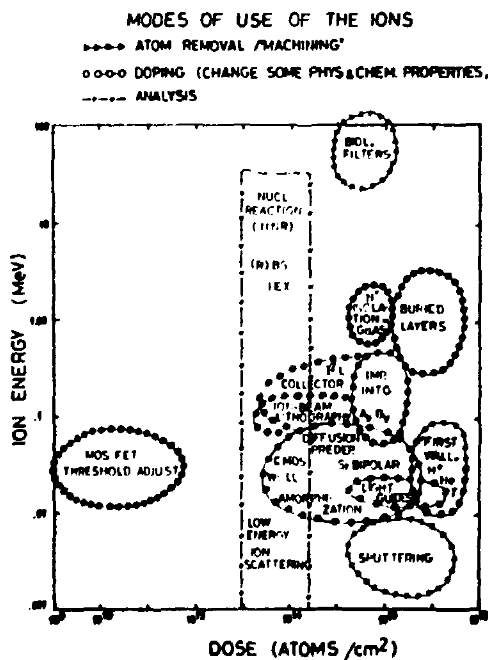

Fig. 1

The first scattering experiment of this type was performed by Geiger and Marsden but the goal was to prove Rutherford's theory of atoms [1]. The inverted question, i.e. to use scattering as an analysis technique, was proposed by Turkevich et al. and led to the first in situ chemical analysis of the lunar surface during the landing of Surveyor. V ([2], *Fig. 2*).

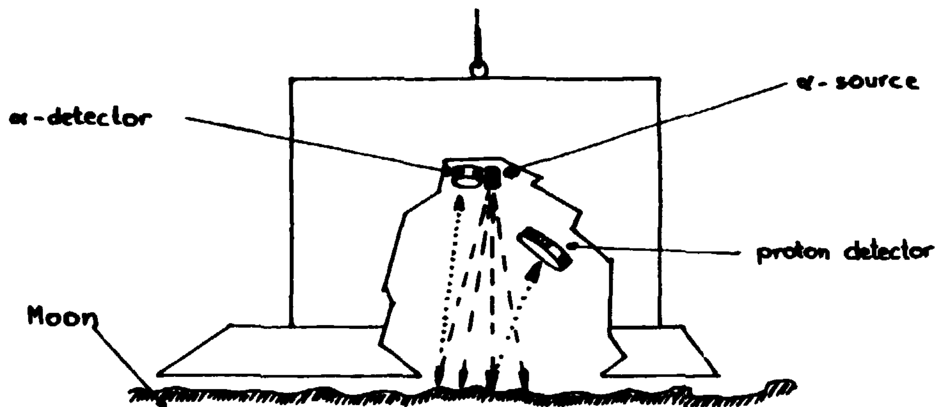

Fig. 2

The use of particle accelerators was the next powerful step made in Chalk River (Canada) and Aarhus (Denmark).

2. BASIC IDEAS

The BS is based on the energy loss during scattering of (light) ions on target atoms. If a monoenergetic beam of ions hits the target, the energy will decrease by elastic scattering (kinematic energy loss) and by non-elastic "steering" collisions with the electron clouds (energy loss by electronic stopping). The first will be connected with masses (chemical-type analysis) and by the second, the location of this scattering atom will be detected (depth-dependent analysis, "profiling"). The total information will contain both chemistry and depth distribution. The so-called nuclear stopping (stopping by nuclear, i.e. elastic collisions) is negligible at these energies. It may cause damage

in the sample about the penetration depth of few microns, bearing no significance in analysis.

If the target is a single crystal, use can be made of the alignment of the well-collimated beam with any crystal axis or plane. In this case atoms in the "shadow cone" of the first ones, will not be visible.

This type of application will be reviewed by I. Steensgaard, in this book.

For detailed discussion of BS, the reader is referred to a book of Chu et al. [3] and references therein.

2.1 Experimental arrangement

To match the above requirements the basic set-up consists of the

accelerator,
analyzing magnet,
beam line and collimator,
goniometer and target,
energy sensitive particle detector,
amplifier,
multichannel analyzer, counting particles
with energy $(E_i, E_i+\Delta E)$
ion current measurement and integration,
vacuum system,
other optionals *(Fig. 3)*

The most commonly used projectiles are $^4He^+$, H^+. For special purposes (see Ch.7) heavier ions, like $^{14}N^+$, $^{16}O^+$ are also useful. Mostly for IINR, deuterons can also be a choice.

The usual geometry (in laboratory system) is the $\theta \approx 170^o$ scattering, i.e. almost total backscattering. Different angles (say, "glancing" incidence and/or exit) are used for near-surface analysis (see Ch.7).

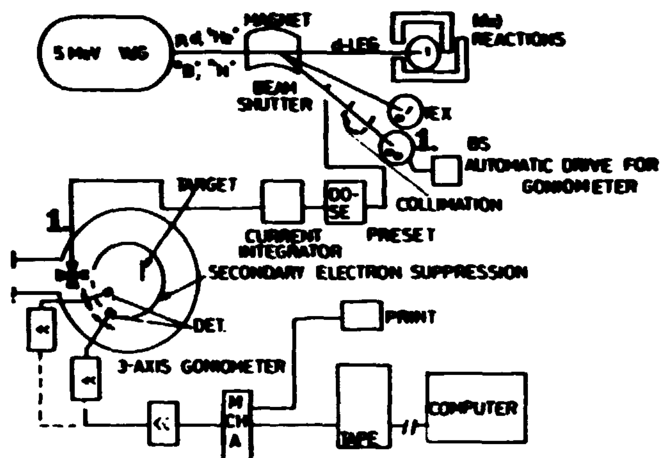

Fig. 3

Beam energies vary in the MeV range, 1-3 MeV is the most commonly applied. The beam diameter is normally about 0.5 mm, but focussing down to the μm range has been achieved. The 10 μm range is quite simple to attain.

Standard parameters lead to a depth-dependent chemical and structural analysis of the top few thousand angstroms of a solid averaging over a 10^{-1} mm^2 area. Typical depth resolution is 150 Å, but if only existence of an impurity is concerned, small fractions of monolayers can be detected (10^{12} atoms/cm^2).

A brief review of sensitivities for different concepts is given on *Fig. 4.* (Dotted lines: for "good" targets, smashed line: qualitative measurement only).

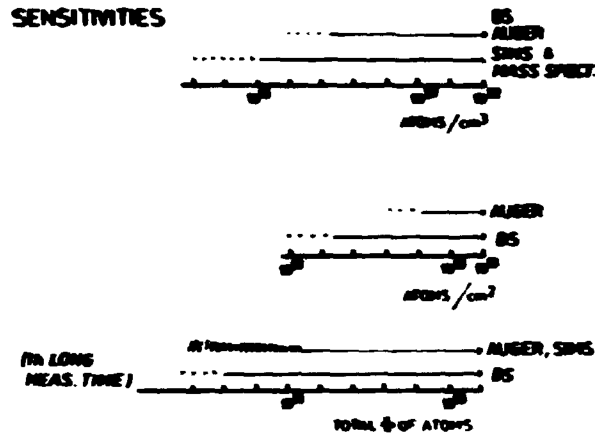

Fig. 4

2.2 Basic formulae

2.2.1 Mass spectrum (Kinematic energy loss)

For a simple collision, the ratio of ion energy (E_o before, E_1 after collision) is a function of masses of projectile (M_1) and target (M_2) and scattering angle (θ, for backscattering $\theta=\pi$)

$$k = \frac{E_1}{E_o} = \left\{\frac{[1-(M_1/M_2)^2\sin^2\theta]^{1/2}+(M_1/M_2)\cos\theta}{1+(M_1/M_2)}\right\}^2$$

$$=\left(\frac{M_2-M_1}{M_2+M_1}\right)^2 \qquad \text{(for } M_2 \quad M_1,\ \theta=\pi\text{)}.$$

This formula shows how the particles "see" different masses:

	C	N	O	Si	Au
$K_{He}^{170^o}$	0.25	0.31	0.36	0.56	0.92

Using these values it is easy to calculate $E_1(=kE_o)$.

2.2.2 Yield (spectrum height) and scattering corss section (σ)

The basic formula for differential cross-section is known since the work of Rutherford.

$$\frac{d\sigma}{d\Omega} = \left(\frac{Z_1 Z_2 e^2}{2E\sin\theta}\right)^2 \frac{\{\cos\theta + [1-(M_1/M_2)^2\sin^2\theta]^{1/2}\}^2}{[1-(M_1/M_2)^2\sin^2\theta]^{1/2}}$$

in a system of reference fixed to the laboratory.

With

$$\sigma \equiv (1/\Omega)\int_{\Omega}(d\sigma/d\Omega)d\Omega ,$$

where Ω is the solid angle of the detector, the total number of detected particles (A) will be

$$A = \sigma\ \Omega\ Q\ Nt .$$

Here Q is the total number of incident particles, N the atomic concentration, t the thickness of the layer probed by the beam (Nt is the areal density of atoms, cm^{-2}).

The A will govern the height of the spectrum detected for a particular energy range.

2.2.3 Depth scale, electronic stopping

Steering collision on electron clouds will also cause energy loss, which will superimpose on kinematic effects. This energy loss can be characterized by a function

$$\frac{dE}{dx} = f(x,E,M_1,M_2)$$

with x the travelled length.

The stopping cross section (ε) is defined as

$$\varepsilon = \frac{1}{N}\ \frac{dE}{dx} .$$

A basic parameter defined in [4] is the energy loss factor, [S].
For particles on the way in

$$x = -\int_{E_0}^{E} \frac{dE}{\left(\frac{dE}{dx}\right)} ,$$

for $\frac{dE}{dx}$ = const. this yield

$$E_0 - x\frac{dE}{dx}\Big|_{IN} = E .$$

For the way out

$$kE - \frac{x}{\cos\theta}\frac{dE}{dx}\Big|_{OUT} = E_1 .$$

As kE_0 is the high-energy edge of the yield vs. energy curve and E_1 is the detected energy, the energy loss

$$\begin{aligned} \Delta E &= kE_0 - E_1 \\ &= [k\frac{dE}{dx}\Big|_{IN} + \frac{1}{\cos\theta}\frac{dE}{dx}\Big|_{OUT}]x \equiv [S]\ x \\ &\approx [k\frac{dE}{dx}\Big|_{E_0} + \frac{1}{\cos\theta}\frac{dE}{dx}\Big|_{kE_0}]x . \end{aligned}$$

The [S] factor converts energy loss into depth. As a basic advantage of BS, the depth scale is more or less linear to a depth of 3-6000 Å and no calibration is needed.

3. HOW TO READ BACKSCATTERING SPECTRA?

Simple spectrum of a monolayer with different atoms contains peaks at energyes $k_{M_i} E_0$ (*Fig 5a*). The height is governed by the energy dependence of σ and, first of all, from the composi-

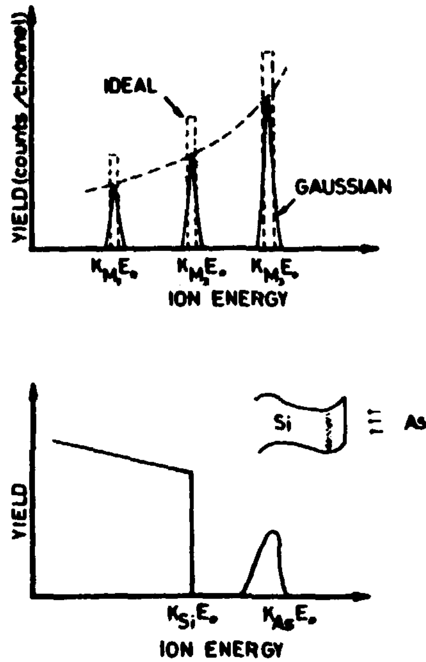

Fig. 5a,b

tion. For a layer of finite thickness, the peaks are converted into pulse-like quadrangles, where information on layer thickness appears as their width. On *Fig. 5b*, spectrum of a semi-infinite solid (Si) implanted with a heavy atom (As) is displayed schematically.

Fig. 6 shows steps of converting a spectrum (two implants, one deep, in silicon) into a from read easily, say, by a metallurgist. One has to make two corrections. The proper value of σ must be used to adjust spectrum height. This yields the real concentration scale. Energy of surface scattering (kE_o) and depth scale, [S], is different for all components (fortunately [S] is about 100 eV/Å). Having absolute scales, the atomic concentration vs. depth profiles can be constructed. It is a big advantage that the spectrum can be evaluated to a reasonable accuracy just by eyeball.

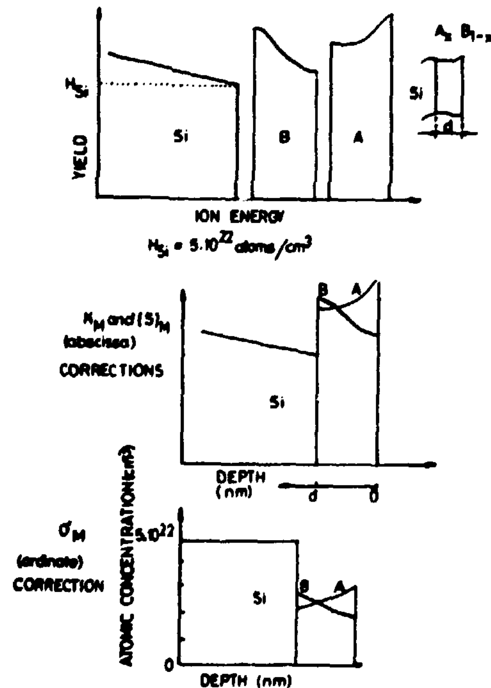

Fig. 6

4. CHANNELING IN CRYSTALLINE MATERIALS

When the incoming beam is aligned with any low-index axis or plane in a crystal, further information can be gained. In this case the conditions for channeling are fulfilled. If the atoms are lined up and the particles can be bounced back by only the first atoms of the channel walls the electronic stopping will steer them down, as shown in a drawing by Ziegler et al. (*Fig. 7*). In this case the yield of BS will decrease to a

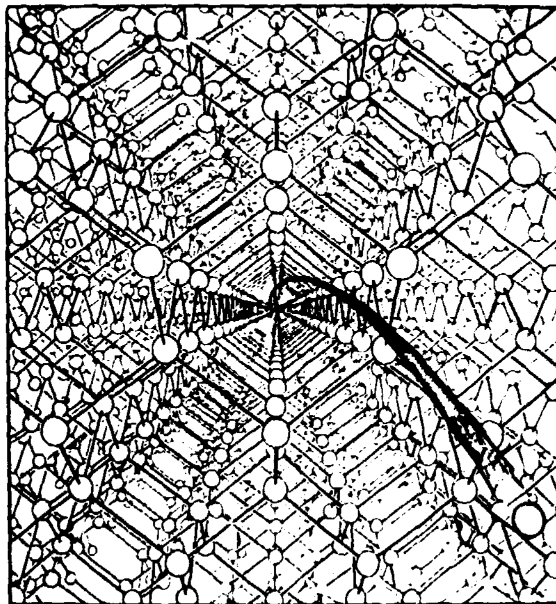

Fig. 7

few per cent of its original non-oriented ("random") value.

4.1 Characteristic quantities for channeling

4.1.1 Half-width at half-minimum (HWHM)

If a detector and a single-channel analyzer is adjusted to have a window for a specific energy (E_1,E+ΔE) corresponding to an atomic species, a tilt-through over a channeled direction

brings information on crystallinity and lattice location of dopants (impurities).

If the window is adjusted to an energy of particles backscattered from near-surface matrix atoms, the yields vs tilt-through curve has a minimum in the channeled direction. The yield there relative to a random (i.e. non-oriented) yield is the minimum yield (χ_{min}). The smaller χ_{min} is, the more perfect is the crystal. If $\chi_{min} \approx 10^{-2}$, backscattering only from surface atoms ($\approx 10^{15} cm^{-2}$) occurs. The HWHM would be characteristic to the "openness" of the channel.

The tilt-through experiment for a substitutional impurity will result in the same curve as of the matrix atoms, except the energy value is different. Altered FWHM value in this case gives information about the exact lattice position and, sometimes the size of the impurity.

An interstitial impurity is visible for any angle of incidence, therefore, the yield will not be influenced by the angle of incidence.

Thus, the tilt-through experiment gives information on crystallinity and substitutionality/interstitialcy of the dopants.

4.1.2 The minimum yield (χ_{min})

If the whole yield vs energy spectrum is measured by a multichannel analyzer, the χ_{min} can also be defined as a ratio of random (matrix) yield and the minimum aligned yield (*Fig. 8*) right behind the so-called surface peak. This peak is caused by the first atomic layer or by some disorder present at the surface. The use in surface analysis will be reviewed here by Stensgaard.

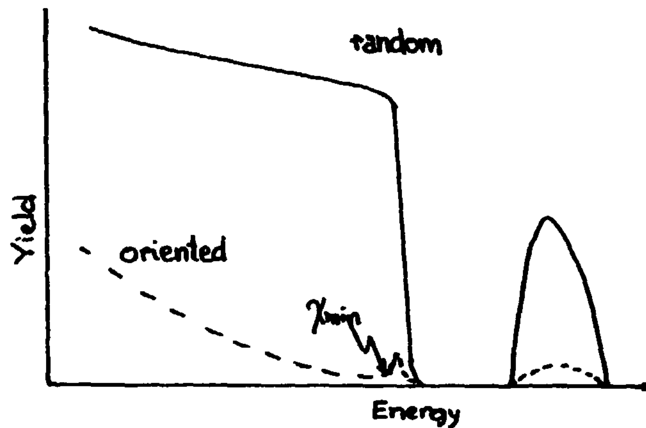

Fig. 8

4.1.3 Critical angle for dechanneling ($\psi_{1/2}$)

This angle characterizes the particles leaving the channels. If the angle between particle trajectory and channel axis exceeds $\psi_{1/2}$ the ion will be scattered out of the channel.

For MeV light ions

$$\psi_{1/2} = \alpha \left(\frac{2Z_1Z_2e^2}{Ed}\right)^{1/2} \qquad 0.8 \leq \alpha \leq 1.2$$

d: lattice constant.

The energy-dependence of $\psi_{1/2}$ gives possibility to find quasi-oriented polycrystals.

4.1.4 Shadow cones

The first atoms in the crystal will define shadow cones by the closest encounters. Atoms lying within this cone will not be visible for BS. This effect is used in surface morphology measurements giving a direct information on surface atoms. This is also reviewed by I. Stensgaard.

4.1.5 Flux peaking

The potential distribution in a channel is not a simple step-function, but is rather of a valley-type. Therefore, particles running along it with non-zero lateral velocity component tend to be focussed in the median of the cannel. As a consequence, if atoms (foreign or matrix) are located in the middle of the channel, the probing ions will hit them with an enhanced probability. This enhanced yield at zero angle is called "flux peaking". Comparing experimental yields with calculations, a model of elementary crystal cell can be deduced (*Fig. 9*) [5].

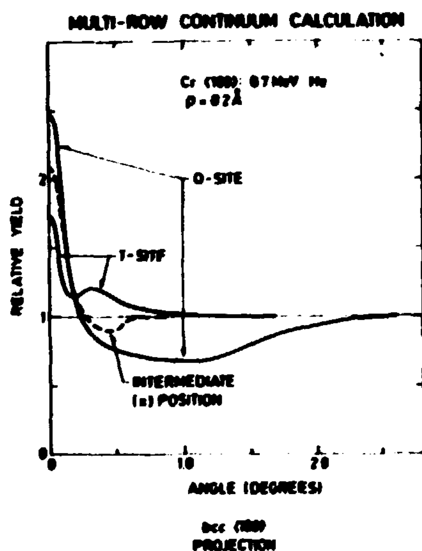

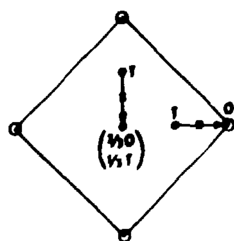

Fig. 9

4.1.6 Triangulation

Triangulation is not really one of the characteristic quantities, but it is a simple and usual way to locate foreign atoms in the lattice. *Fig. 10* shows a diamond lattice with one substitutional foreign atom (white ball) and a tetrahedral interstitial (cube), viewed from a random direction. In principle all atoms are exposed to the beam, i.e. their signal appears in the spectrum (*Fig. 11* shows the case in two dimensions).

Looking down in the <111> or <100> directions (<100> on *Fig. 12*), both substitutional and the above tetrahedral interstitials fall into the shadow cone of a crystal atom. From this direction the yield for these impurities drops (*Fig. 11*, ∎ and □ from <11> direction).

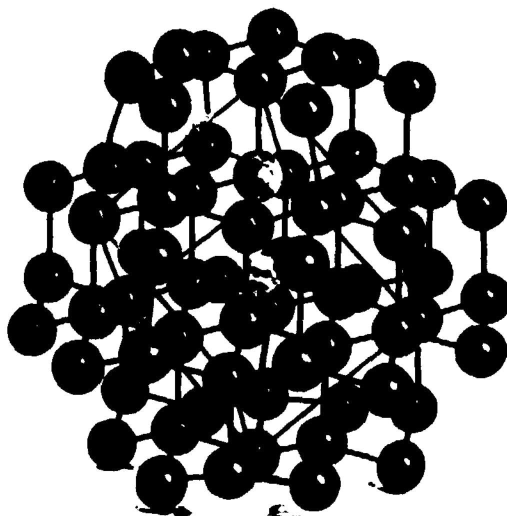

Fig. 10

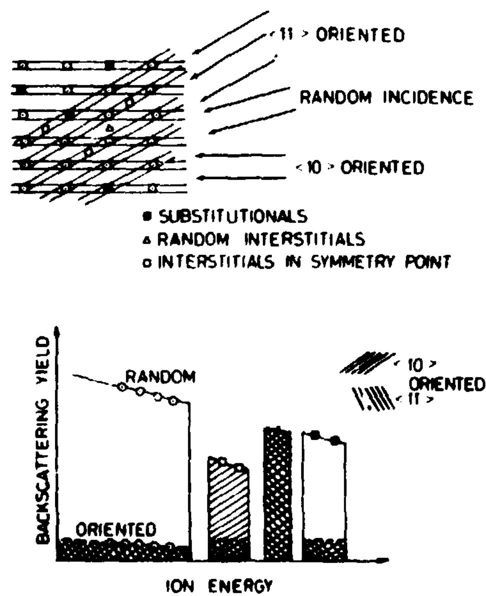

Fig. 11

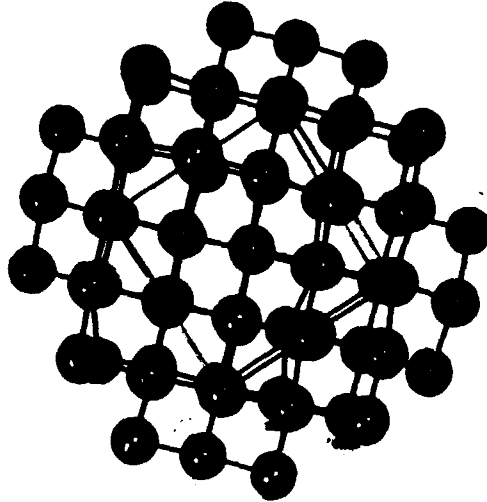

Fig. 12

For substitutionals this is the case far all directions, but there exist directions, where the interstitials even in symmetry point can be made visible (*Fig. 13*,<110>; and <10> on *Fig. 11*).

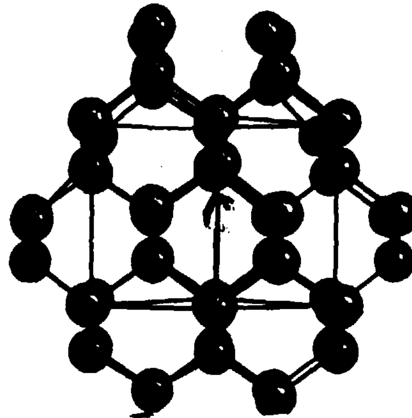

Fig. 13

Triangulation thus is a powerful tool to locate atoms in the lattice.

5. DEFECT CHARACTERIZATION

In the previous discussion no assumption was made that the locate. atoms were of different quality. In principle, dislocated matrix atoms can also be visible adding signal to the channeled spectrum. This superposition character limits the sensitivity of BS in defect characterization.

A defect may cause
- direct backscattering,
- increased minimum yield,
- enchanced dechanneling.

Recent results (see e.g. [3], Ch8)

dislocations themselves cause no backscattering
but show √E-dependent enhanced
dechanneling (*Fig. 14*,[6]),

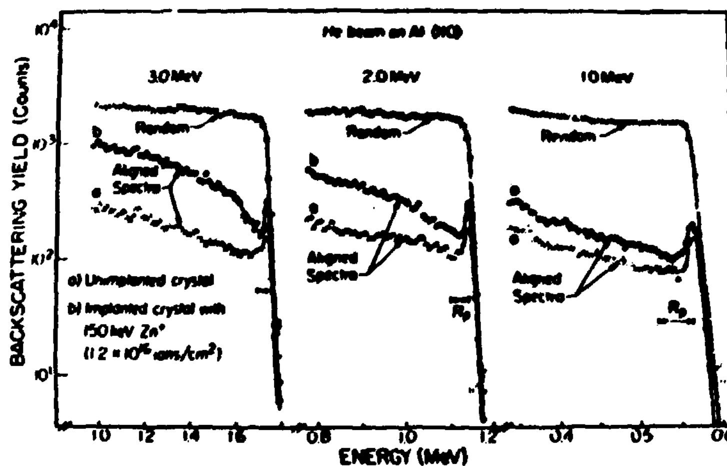

Fig. 14

stacking faults increase minimum yield,
but do not influence dechanneling,

twin crystals show good channeling
in twin direction (<511> for Si, *Fig. 15*)

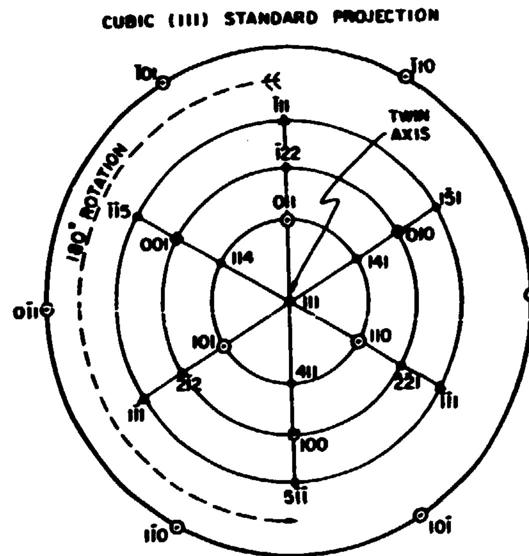

Fig. 15

quasi-oriented polycrystals show improved
χ_{min} at lower beam energies.

At this point it is advisable to show experimental examples to illustrate the previously mentioned.

6. EXAMPLES

6.1 Thin film analysis

Composition of thin films were determined back in 1970 ([7] *Fig.16*). An analysis according to 2.2 yielded depth-dependent composition of Si_xN_y layers. *Fig. 16 b* shows that a failure in end polishing before CVD nitride deposition also became obvious.

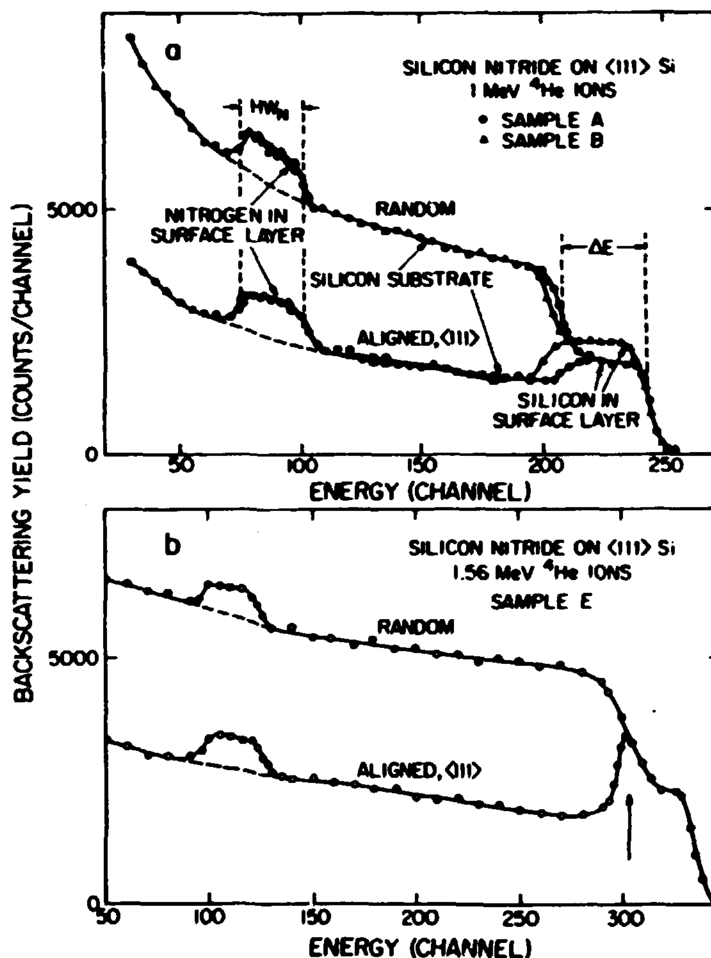

Fig. 16

For different ammonia-to-silane ratios during deposition, chemical composition and mechanical density were determined (*Fig.17*)[8].

Thin film analysis by BS is a straightforward way to check thicknesses, composition. Measurements are even fast(10 min/sample) (*Fig. 18*,[9], *Fig. 19* [20]). *Fig. 19* shows an ion-beam mixing experiment, i.e. where chemical reaction is motivated by the kinetic energy of an implanted atom (χe).

Diffusion in a thin surface layer can also be detected by BS [11]. On *Fig. 20* a diffused antimony profile can be seen starting from an implanted predeposition.

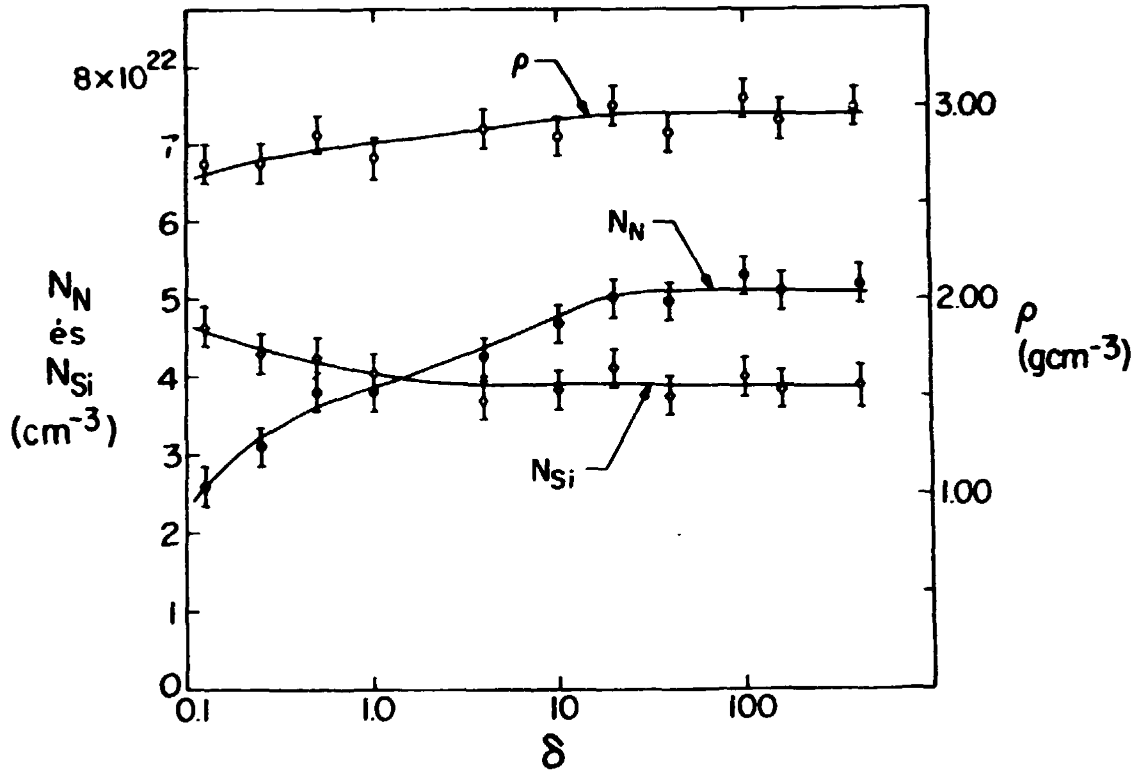

Fig. 17

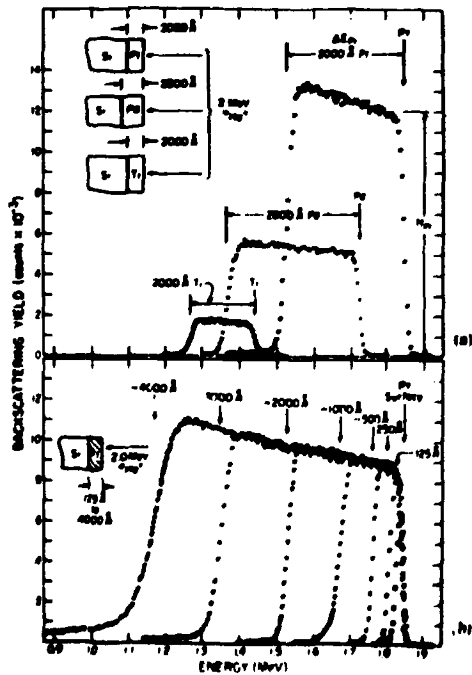

Fig. 18

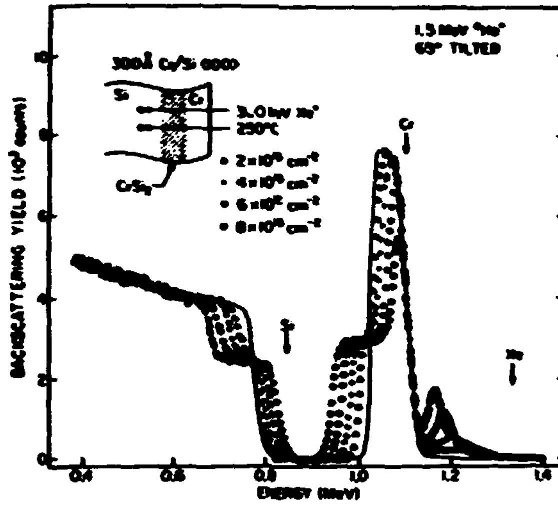

Fig. 19

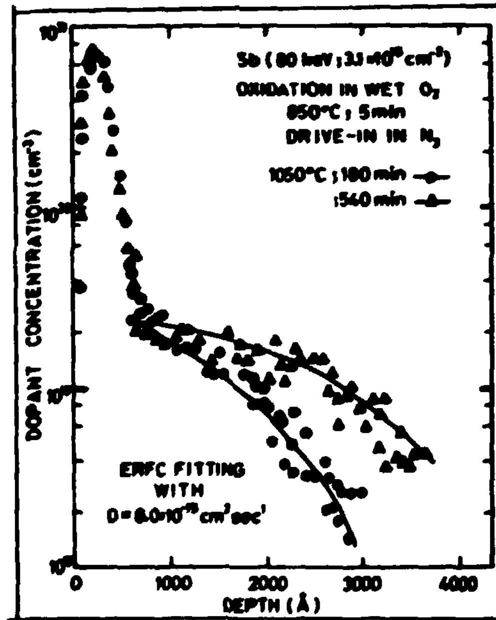

Fig. 20

6.2 Lattice location

There are numerous examples that could have been selected to show the power of triangulation etc. We pick only three results to show specificity. *Fig. 21* [12] shows depth-dependent lattice location of Se in Si. Random and aligned Se-peaks coincide in the near-surface region detecting random distribution of Se. At greater depth, however, the curves differ indicating

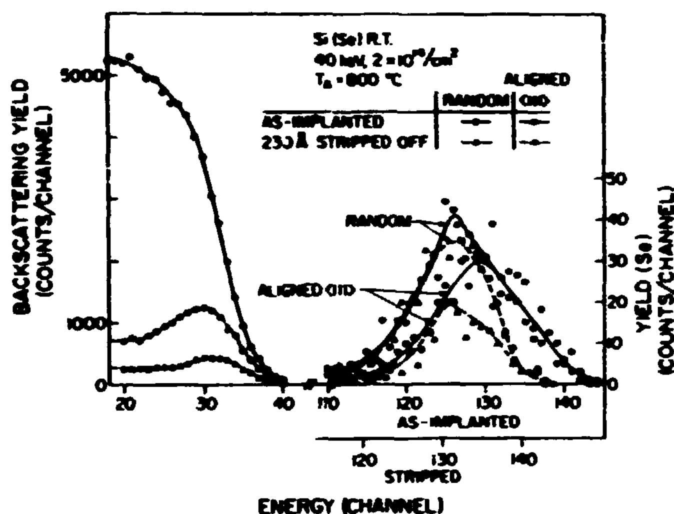

Fig. 21

about 50% substitutionalty of Se. An anodic stripping proved that this was not an artefact.

Based on *Fig. 20* oriented spectra were also taken. This showed that part of the implanted antimony in the peak also occupies lattice sites. *Fig. 22* shows that first the intersitials diffuse in $((N_R'-N_A')/(N_R'+N_R'')$ being characteristic to substitutional Sb [13]).

Fig. 23 [14] shows proof that gold is not a substitutional alloy in GaAs.

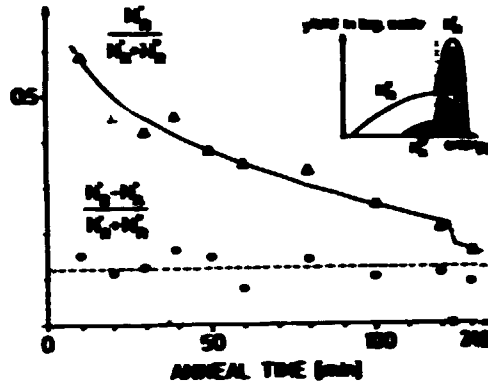

Fig. 22

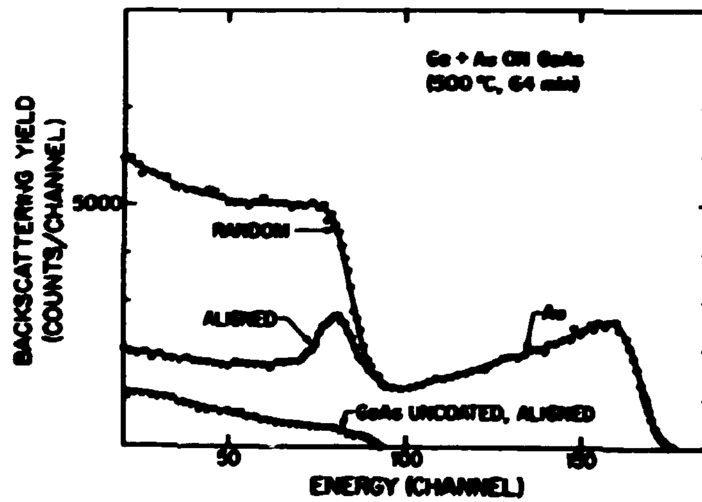

Fig. 23

6.3 Lattice disorder characterization

The aim of gold alloying on GaAs was to produce good ohmic contacts [14]. *Fig 24* shows that prolonged annealing increases lattice damage without really influencing the Au distribution.

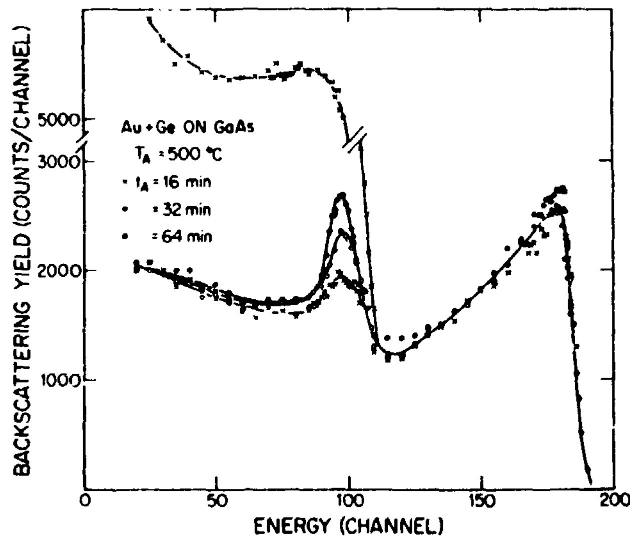

Fig. 24

Characterization of dislocations in Al was shown on *Fig. 14*. If a dislocation network is located below the surface, BS can detect it (*Fig. 25* [15]). After a destructive thinning procedure the transmission electron microscopy can reveal the actual picture (*Fig. 26*).

Backscattering spectrometry helped to understand details of epitaxial regrowth of amorphous films and led to a technique of "perfect doping". First the orientation dependence of rate of regrowth ($V_{110}>V_{100}>V_{111}$) was found (*Fig. 27* [16]). Then the perfect regrowth of <100> Si (*Fig. 28* [17]) and the low--temperature implantation doping (*Fig. 29* [18])led to perfect doping. In this case the epitaxial regrowth incorporates the implanted phosphorus.

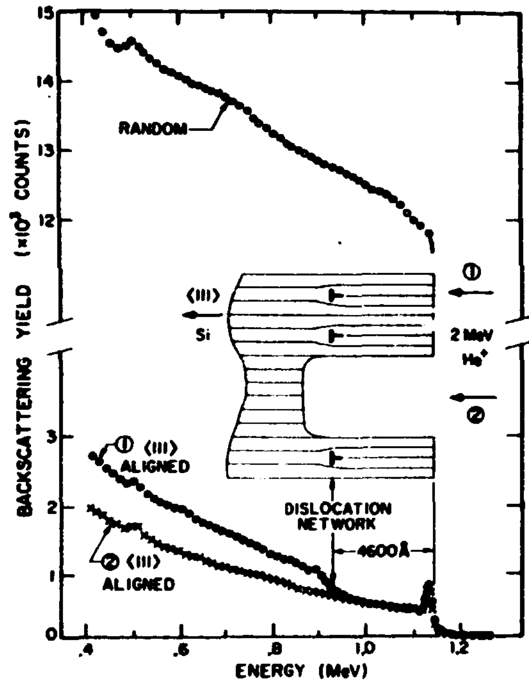

Fig. 25

Fig. 26

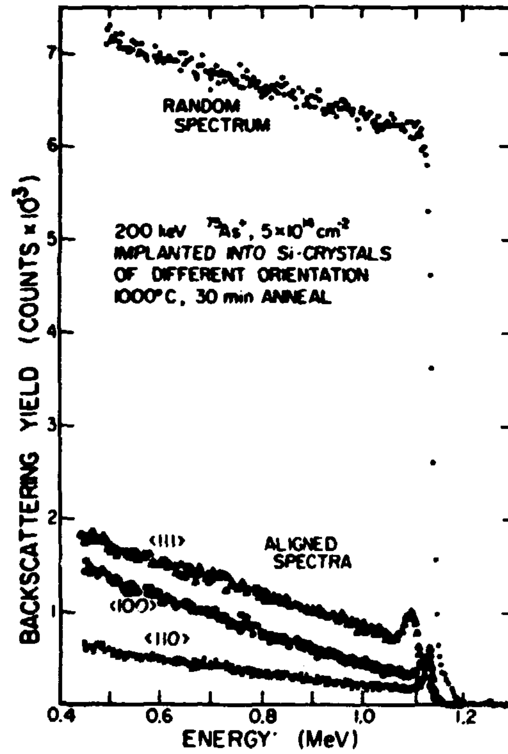

Fig. 27

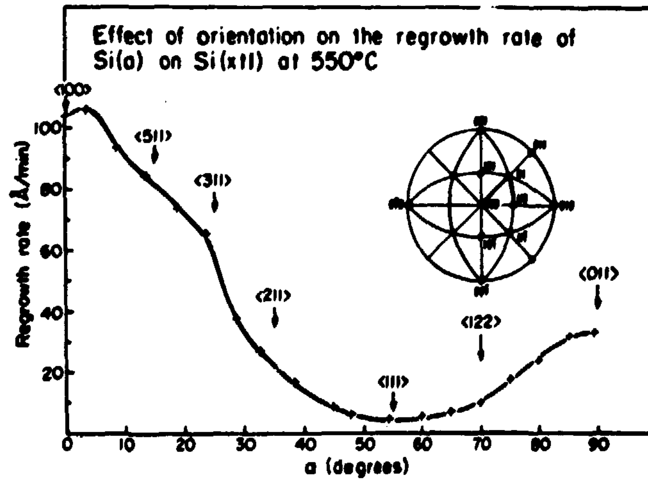

Fig. 28

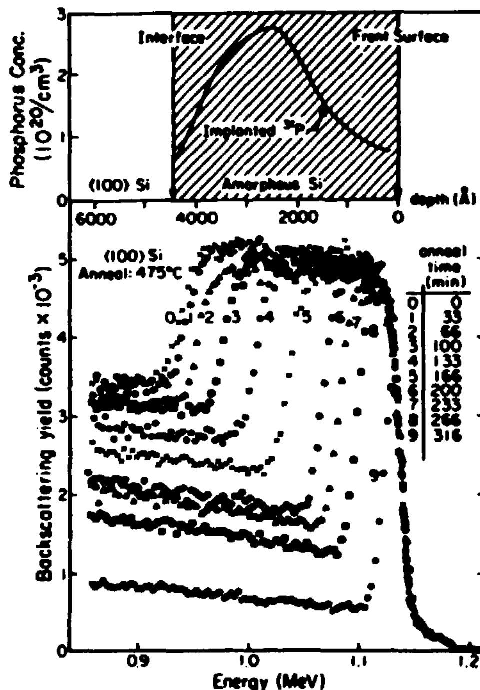

Fig. 29

The next examples shows the improvement of crystalline quality of silicon grown on Al_2O_3 (SOS). *Fig. 30* gives (probably the first) example of BS analysis of SOS [19]. Aligned spectra show enhanced dechanneling which indicates the presence of mechanical stresses. For years there wasnot any significant improvement in technology (*Fig. 31*, curve 2), but a deep channeled implant which left the surface undamaged, followed by one epitaxial regrowth from the top, leads to aperfect interface [20]. Circuits produced in this layer have an order of magnitude lower leakage current cross-sectional TEM-picture for comparison is to be seen on *Fig. 32*.

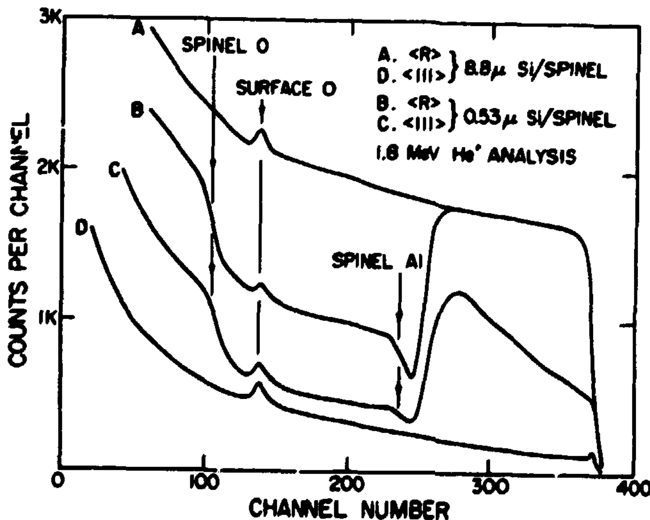

Fig. 30

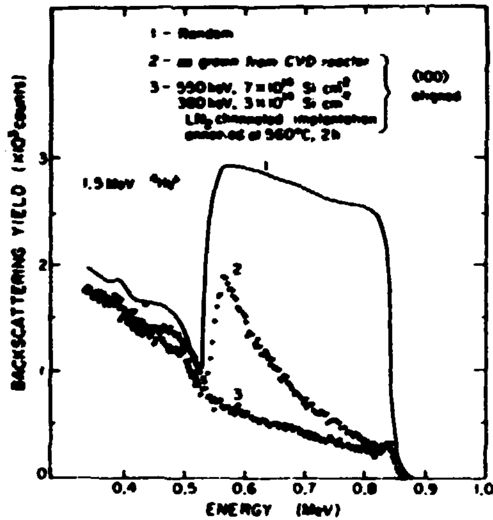

Fig. 31

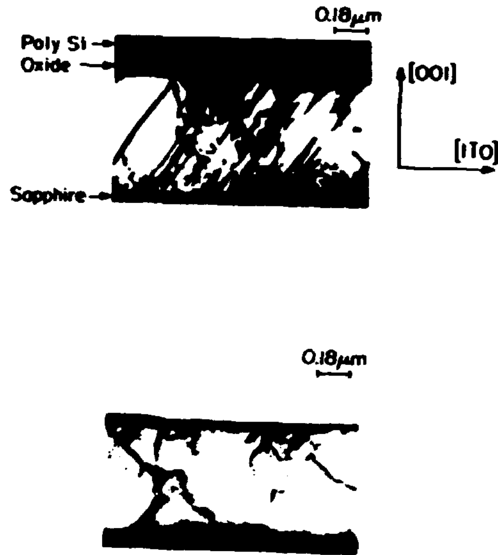

Fig. 32

7. FURTHER "TRICKS"

The possibilities of BS do not exhaust with the above reasonably "good" problems. There are numerous ideas to handle difficult structures. Options for optimalization are the type of projectile, energy, scattering geometry, combination with layer removal (preferentially with anodic stripping). Added to these are nuclear reactions, IEX and ion focussing.

Heavier projectiles, such as $^{12}C^+$, $^{14}N^+$, $^{16}O^+$ increase sensitivity, but can damage the detector and penetration is shallower. The best application for this technique is the quantitative determination of submonolayer coverage on a light-mass substrate. In this case BS beats also SIMS, because the latter consumes the substrate and passes very fast over the surface layer. Total number of a few million atoms can be measured quantitatively [21].

Energy of the projectile is one more free parameter. Higher energy will separate near-masses, but compresses the depth scale.

At lowest energies a new method, the low-energy ion scattering is reviewed separately by D. Karpuzov (in this volume).

More attention was paid recently to the optimalization of geometry. If improvement of depth resolution is essential, the glancing angle geometries help, because the beam probes a $\{\frac{1}{\cos\Theta_1} + \frac{1}{\cos\Theta_2}\}$-times longer distance in the sample. Therefore, the energy losses are greater for the same vertical distances [22]. The different possible geometries, which make also use of channeling are summarized on *Fig. 33* [23a]. It is to be seen that a glancing exit in itself could be useful ([23b], *Fig. 34*). It can be seen on this comparison of "regular" and glancing exit spectra that while the regular BS only shows a partially disordered surface layer, the glancing exit spectrum reveals that this surface layer is thin, bit still fully amorphous.

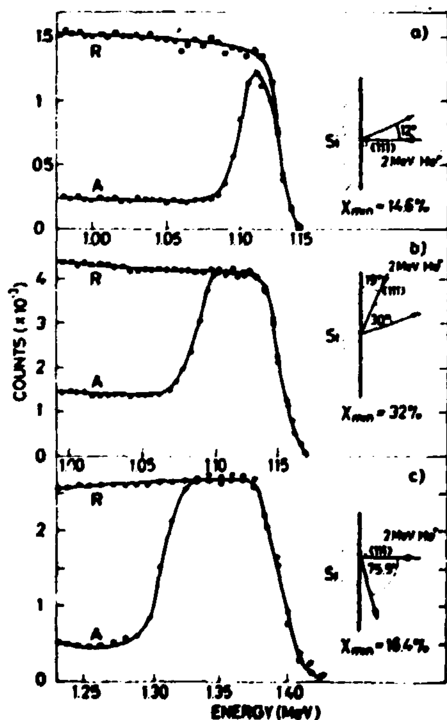

Fig. 33

Sensitivity can be raised for special atoms by making use of (αα) reactions, i.e. of the so-called resonance of Rutherford scattering.

One of the most useful one is the 3.045 MeV resonance of He^+ on oxygen atoms. To use this as an analytical tool was proposed in [24] and quantitative discussions are described in [25]. The $\sigma_{res} = 17\sigma$, therefore, an equal increase in sensitivity is found, making possible e.g. quantitative analysis of native oxides on heavy substrates (*Fig. 35*, [26]). By stepwise increasing the projectile energy, the condition for resonance will be

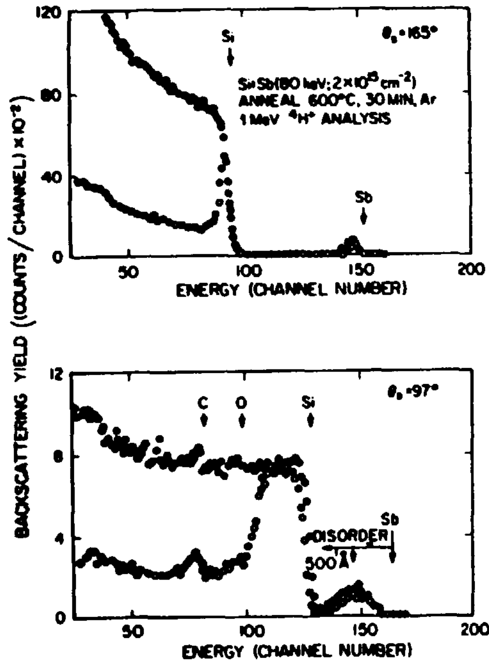

fulfilled deeper and deper, thus the beam will probe greater depths (*Fig. 36*,[27]) for oxygen.

Combination of (αα) resonance and glancing angle scattering still increases sensitivity, both in depth resolution (down to 50=100 Å) and atomic sensitivity (additional factor 3.5) [28].

A further trick is ion focussing. A focussing system to about 10 μm is easy to achieve, but beam diameter of 1-2 μm can be reached by some sophistication [29].

Fig. 34

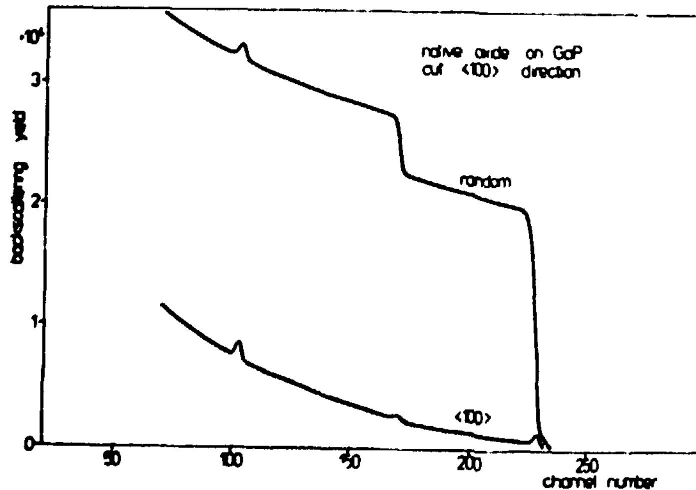

Fig. 35

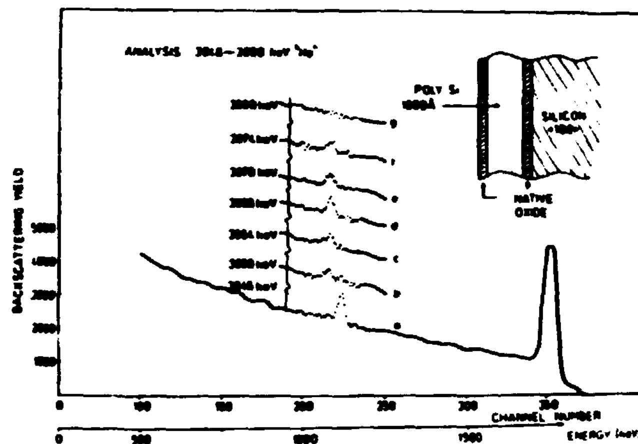

Fig. 36

8. HOW BS HELPS OTHER TECHNIQUES?

BS was used in the recent years probably in the widest range of promlems ever attacked by a single method. The diversity of information from one measurement and the non-destructiveness and, even sometimes, relatively short measuring time compensates for usual lack of microstructural information.

A major advantage of BS that it's free from artefacts as opposed to e.g. SIMS, Auger, where problems of sputtering, ionization make quantitization tough. BS can check sputtering to screen out preferential sputtering or helps SIMS to be quantitative. After this check, the sensitivity of SIMS can be safely used. A counter--example is shown on *Fig. 37* [30].

Why electron microscopy may need BS? As it was pointed out, BS is essentially non-destructive, while transmission electron microscope needs thin (transparent) samples. This is a destructive procedure. What BS can say aforehand, whether the microscope will find defects, or the sample is practically perfect.

As conclusion, because of some ambiguity of the concept "sensitivity", we'd rather summarize the types of problems, where BS is probably the winner.

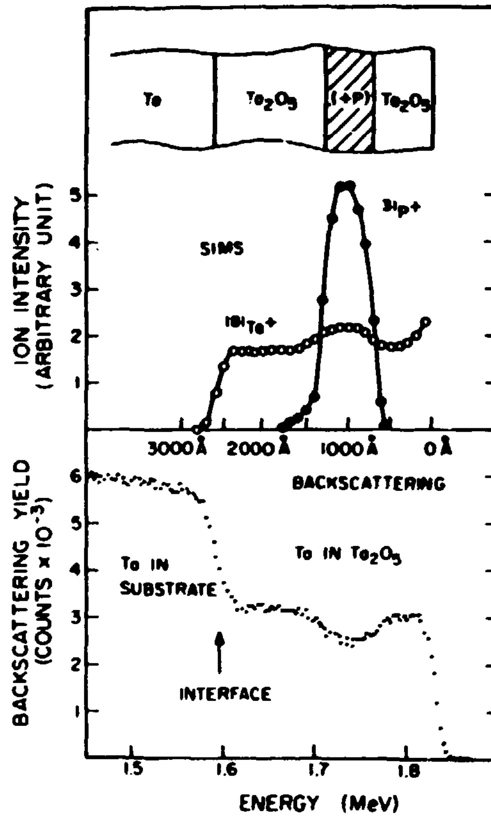

Fig. 37

1/ Metallurgy (composition alloying reactions, phase diagrams) of thin films

10 min/sample

2/ Diffusion of heavy atoms (As,Sb)

Direct profiles

3/ Special (heavy) impurities and their location above 10^{12} cm^{-2} concentration

(in 45 min overall picture, in 90 min full picture is possible)

4/ Collapse of metastable systems (metal or semiconductor)

(30 min/measurement)

5/ Depth dependence of defects and
characterization (machine time between 30-100 min)

6/ Calibration, quantification of implantation,
or other analytical methods

7/ Traces of oxygen in thin layers
(could be time-consuming)

8/ Submonolayer coverage, adsorption
on crystalline surfaces
(more direct than LEED, no model ambiguity)

9/ Sputtering measurements.

Presumably this is convincing enough.

* * *

Thanks are due to Drs. P. Revesz and G. Mezey for commenting the manuscript.

REFERENCES

[1] Geiger, H., E. Marsden, Phil.Mag. 25, 606 (1913)

[2] Turkevich, A.L. et al. in Surveyor Project Final Report, II. pp. 303-387 (JPL., Pasadena, California)

[3] Chu, W-K., J.W. Mayer, M-A. Nicolet: Backscattering Spectrometry (Academic Press, N.Y., 1978)

[4] Meyer, O., J. Gyulai, J.W. Mayer, Surf.Sci., 22, 263 (1970)

[5] Vook, F.L., S.T. Picraux in Radiation Effects on Solid Surfaces (Ed.M. Kaminsky, Amer. Chem.Soc. 1976) p. 308

[6] Foti, G., S.T. Picraux, S.V. Campisano, E. Rimini, R.A. Kant in Ion implantation in semiconductors (Eds. F. Chernow, J.A. Borders, D.K. Brice, Plenum, 1977) p.247

[7] Gyulai, J., O. Meyer, J.W. Mayer, V. Rodriguez: Appl.Phys. Lett. 16, 232 (1970)

[8] Gyulai, J., O. Meyer, J.W. Mayer, V. Rodriguez: J.Appl.Phys. 42, 451 (1971)

[9] Chu, W-K., J.W. Mayer, M-A. Nicolet, T.M. Buck, G. Amsel, F. Eisen Thin Solid Films 17, 1 (1973)

[10] Lau, S.S., Tsaur, B.Y. in Thin Film Interfaces and Interactions (Eds. J.S.S. Baglin, J.M. Poate The Electrochem Soc, Princeton 1980) p. 205

[11] Gyulai, J., L. Csepregi, T. Nagy, J.W. Mayer, M. Müller: Le Vide No 184, 416 (1974)

[12] Gyulai, J., R.D. Pashley, J.W. Mayer: Rad.Eff. 7, 17 (1971)

[13] Kotai, E.: Ph.D. Thesis, Eötvös Univ. Budapest, 1977

[14] Gyulai, J., J.W. Mayer, V. Rodriguez; H.J. Gopen, A.Y.C. Yu: J. Appl.Phys. 42, 3578 (1971)

[15] Tseng, W.F., J. Gyulai, S.S. Lau, J. Roth, T. Koji, J.W. Mayer: Nucl.Instr.Meth. 149, 615 (1978)

[16] Müller, H., W-K. Chu, J. Gyulai, J.W. Mayer, T.W. Sigmon, T.R. Cass: Appl.Phys.Lett. 26, 292 (1975)

[17] Csepregi, L., E.F. Kennedy, J.W. Mayer, T.W. Sigmon: J.Appl.Phys. 49, 3906 (1978)

[18] Kennedy, E.F., L. Csepregi, J.W. Mayer, T.W. Sigmon: J.Appl.Phys. 48, 4241 (1977)

[19] Gyulai, J., I.V. Mitchell, V. Rodriguez, J.W. Mayer: Proc.Int.Conf. on Phys. and Chem. of Semiconductor Heterojunctions (Budapest, V-293 (1970))

[20] Lau, S.S., S. Matteson, J.W. Mayer, P. Revesz, J. Gyulai, J. Roth, T.W. Sigmon, T. Cass: Appl. Phys.Lett. 34, 76 (1979)

[21] Dearnaley, G., G.M. McCracken, J.F. Turner, J. Vince: Nucl.Instr.Meth. 149, 253 (1978)

[22] Williams, J.S.: Nucl.Instr.Meth. 126, 205 (1975)

[23] a, Williams, J.S.; Nucl.Instr.Meth. 149, 207 (1978)
b, Mezey, G., E. Kotai, T. Lohner, T. Nagy, J. Gyulai, A. Manuaba: Nucl.Instr.Meth. 149, 253 (1978)

[24] Keszthelyi L., I. Demeter, G. Mezey, Z. Szőkefalvi-Nagy, L. Varga: Proc.Int.Conf. on Ion Implantation, 1972, Rossendorf (GDR), Zfk-236, p.111

[25] Mezey, G., J. Gyulai, T. Nagy, E. Kótai, A. Manuaba in Proc.Int.Conf. on Ion Beam Analysis (Eds. O. Meyer, G. Linker, F. Kappeler; Elsevier, 1976) p.303

[26] Somogyi, M., M. Farkas-Jahnke, G. Mezey, J. Gyulai: Thin Solid Films 60, 377 (1979)

[27] Mezey, G., M. Somogyi, C.A. Evans, T. Nagy, J. Gyulai in Proc. 7th Int.Vac.Congress (Eds. R. Dobrozemsky, F. Rüdenauer, F.P. Viehböck, A. Breth, Tech.Univ. Wien, 1977) p.571

[28] Kótai, E., G. Mezey, T. Lohner, A. Manuaba, F. Pászti, J. Gyulài: Nucl.Instr.Meth. (accepted, 1981)

[29] Allen, C.R. G. Dearnaley, N.E.W. Hartley, in Ion Beam Surface Layer Analysis (Eds. O. Meyer, G. Linker, F. Kappeler, Plenum, 1976) Vol.2. p. 901

[30] Chu, W-K, M-A. Nicolet, J.W. Mayer, C.A. Evans: Anal.Chemistry 46, 2136 (1974)

Kiadja a Központi Fizikai Kutató Intézet
Felelős kiadó: Krén Emil
Szakmai lektor: Révész Péter, Mezey Gábor
Nyelvi lektor: Révész Péter
Példányszám: 490 Törzsszám: 81-90
Készült a KFKI sokszorosító üzemében
Felelős vezető: Nagy Károly
Budapest, 1981. február hó